Appl. Phys. B 80, 133–138 (2005)
DOI: 10.1007/s00340-004-1619-y

**Applied Physics B**
**Lasers and Optics**

A.A. KOSTEREV✉
Y.A. BAKHIRKIN
F.K. TITTEL

# Ultrasensitive gas detection by quartz-enhanced photoacoustic spectroscopy in the fundamental molecular absorption bands region

Rice Quantum Institute, Rice University, Houston, TX 77251-1892, USA

**Received: 16 July 2004**
**Published online: 1 September 2004 •** 

**ABSTRACT** A trace gas sensor based on quartz-enhanced photoacoustic spectroscopy with a quantum cascade laser operating at 4.55 μm as an excitation source was developed. The sensor performance was evaluated for the detection of $N_2O$ and CO. A noise-equivalent ($1\sigma$) sensitivity of 4 ppbv $N_2O$ with 3 s response time to $(1-1/e)$ of the steady-state level was demonstrated. The influence of the relevant energy transfer processes on the detection limits was analyzed. Approaches to improve the current sensor performance are also discussed.

**PACS** 42.62.Fi; 43.35.Sx

## 1 Introduction

Quartz enhanced photoacoustic spectroscopy (QEPAS) first reported in 2002 [1] is a technique that potentially allows quantification of trace species in extremely small gas samples ($< 1\,\mathrm{mm}^3$). This unique capability can be particularly useful in microbiological and entomological [2] studies. QEPAS is also suitable to be the basis of the portable gas sensors for field and industrial applications, because this technique has proved to be highly immune to environmental interference such as acoustic noise. The small size of the QEPAS absorption-sensing unit ($\sim 5$ mm typical dimensions) permits convenient integration with semiconductor laser sources such as laser diodes, quantum cascade (QC) and interband cascade (IC) lasers.

QEPAS was successfully applied to ammonia detection at $< 1$ ppm levels using a telecommunication DFB diode laser at 1.52 μm [3]. A number of other species such as $H_2O$, $CO_2$, $C_2H_2$ have also been detected using QEPAS with a widely tunable near-IR diode laser source (AltoWave3500, Intune Technologies) [4]. The best sensitivity to absorption achieved to date with QEPAS is $D(\mathrm{NH_3}) = 7.2 \times 10^{-9}\,\mathrm{cm^{-1}W/\sqrt{Hz}}$, as measured for ammonia at 50 Torr total pressure. Here $D$ is determined as

$$D = \frac{\alpha_{\min} P}{\sqrt{\Delta f}} \tag{1}$$

where $\alpha_{\min}$ is the absorption coefficient corresponding to the noise-equivalent signal, $P$ is the optical excitation power and $\Delta f$ is the detection bandwidth. $D$ strongly depends on the energy transfer processes in the gas, which will be discussed in Sect. 3 in more detail. Variations of $D$ however were found not to exceed a factor of two for the investigated optical transitions in the overtone region. Advances in quantum electronics provided equally powerful spectroscopic sources such as QC and IC lasers for the mid-IR region. The principal purpose of this work was to explore the applicability of QEPAS to the detection of different trace gas species in the mid-IR region of fundamental vibrational absorption bands. Since molecular absorptions in this region are typically $\sim 100$ times stronger than in the near-IR, concentrations $\sim 1$–$10$ ppb should be detectable if $D$ does not change significantly. A QC laser operating at 4.55 μm was provided by Alpes Lasers [5].

The molecules selected for this study were $N_2O$ and CO. Detection of trace concentrations of each of these species is of practical importance for a number of applications. $N_2O$ is an important contributor to the global greenhouse effect [6–10]. Background concentration of nitrous oxide in the atmosphere ranges from 310 to 320 ppbv and increases with an average rate of 0.8 ppb/year [11].

CO constitutes the largest fraction of the pollutants found in industrial and urban atmospheres. It is produced primarily by the incomplete combustion of organic materials and also results from industrial processes and motor vehicles exhausts [12]. Background levels of CO found in relatively unpolluted air range from 0.2 to 1.0 ppmv [6, 12]. CO in exhaled human breath (400–300 ppbv) is an essential biomedical marker for noninvasive disease diagnostics in medicine [13].

## 2 Experimental details

A configuration of the laboratory QEPAS-based gas sensor is shown in Fig. 1. A continuous wave (cw), distributed feedback (DFB) QC laser was used as a photoacoustic excitation source. The laser was liquid nitrogen cooled and covered the spectral range of 2198.3–2195.5 $\mathrm{cm^{-1}}$ when its current was changed from the threshold at 317 mA to 650 mA. The laser radiation was collected with a 13 mm focal length aspherical lens $L_1$, positioned so that the source was imaged at 97 cm from the lens. Such a long refocusing distance re-

✉ Fax: +1-713/348-5686, E-mail: akoster@rice.edu

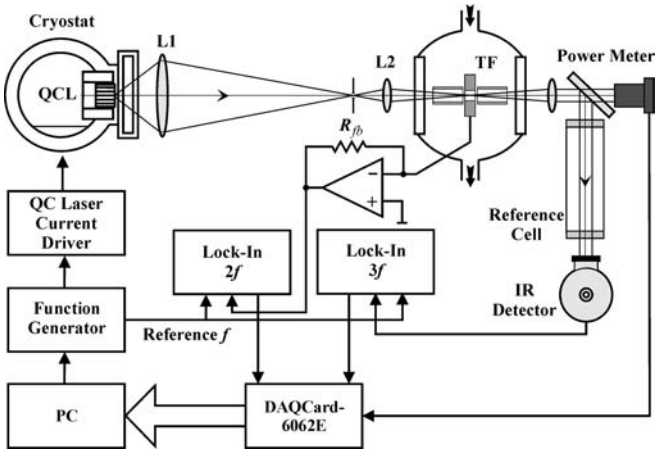


**FIGURE 1** Schematic of the QEPAS trace gas sensor using a QC-DFB laser as an excitation source

duced the spherical aberration and allowed spatial filtering to be performed. A second lens $L_2$ (focal length 5 cm) re-imaged the source between the prongs of the quartz tuning fork (TF). An acoustic microresonator consisting of two fused silica tubes, each 2.45 mm long with a 0.32 mm inner diameter, was aligned perpendicular to the TF plane for sensitivity enhancement [1–4]. Care was taken to prevent the laser radiation from illuminating the microresonator walls. Such irradiation was found to result in a background photoacoustic signal because of radiation absorption in the microresonator silica tubes. The gas cell with $\sim 1\,\mathrm{cm}^3$ volume containing the TF is described in further detail in [3]. The laser beam was recollimated upon exiting the TF cell. A beamsplitter was introduced to deflect a portion of the radiation to the IR detector, while most of the radiation passed to a power meter. A reference cell ($l = 13$ cm) was filled with a high concentration of the species under study (5%–10% peak absorption) for spectral reference.

The QC laser wavelength was modulated at a frequency $f = f_0/2$, where $f_0$ is the resonant frequency of the TF, and the detection of photoacoustic signal was performed at $f_0$, similar to [1–4]. The modulation was implemented by adding a sinusoidal component (typically $\sim 4$ mA peak-to-peak) on top of the dc laser current. The QEPAS experiments were carried out in two modes:

1. Scan mode. In this mode the dc component of the laser current was slowly tuned so that the central laser frequency swept over the desired spectral range.
2. Lock mode. The QC laser current was initially set to make the laser wavelength close to the absorption line center. The $3f$ component of IR detector signal $A_{3f}$ was measured and a proportional correction to the dc component of the laser current $\Delta I = \mathrm{const} \times A_{3f}$ was periodically made to maintain $A_{3f} = 0$. Thus, the laser wavelength was locked to the center of the targeted optical absorption line.

The TF generated piezoelectric current was converted to a voltage using a transimpedance amplifier with a feedback resistor $R_{\mathrm{fb}} = 10\,\mathrm{M}\Omega$. The outputs of the two lock-in amplifiers and other analog signals such as readings of pressure and gas flow meters were digitized using a PCMCIA data acquisition card (National Instruments DAQCard-6062E), which transferred the data to a notebook PC computer. LabView based software provided computer control of the function generator (which in turn controlled the laser current) and the required data acquisition and processing.

Prior to each run of photoacoustic measurements the resonant frequency $f_0$ and $Q$-factor of the TF were determined. In order to do so, the ac voltage from the function generator was applied directly to the TF. The TF current was measured as a function of the applied voltage frequency. An example of the resonance curve is shown in Fig. 2. The parameters $f_0$ and $Q$ depend on the gas pressure, major gas chemical composition, and the temperature. If the gas pressure and composition were maintained constant, the daily drift of $f_0$ did not exceed $\pm 0.02$ Hz. The resonant curve allows the determination of the TF impedance as a ratio of voltage and current. The impedance is purely resistive at resonance, and its value R is related to the thermal noise of the TF:

$$\frac{\sqrt{\langle V_{\mathrm{N}}^2 \rangle}}{\sqrt{\Delta f}} = R_{\mathrm{fb}} \sqrt{\frac{4 k_{\mathrm{B}} T}{R}} \tag{2}$$

where $\sqrt{\langle V_{\mathrm{N}}^2 \rangle}$ is the RMS voltage noise observed at the transimpedance amplifier output, $\Delta f$ is the detection bandwidth ($\Delta f = \frac{1}{2\pi\tau}$, where $\tau$ is the lock-in amplifier time constant), and $T$ is the TF temperature. Other equivalent electrical parameters of the TF ($L$ and $C$) can be found using the equations:

$$2\pi f_0 = \sqrt{\frac{1}{LC}}, \quad Q = \frac{1}{R}\sqrt{\frac{L}{C}} \tag{3}$$

Typically, the $Q$ is 10 000 to 13 000 and $R \approx 90\,\mathrm{k}\Omega$ in air or nitrogen at atmospheric pressure.

To detect the $N_2O$, P(30) transition of the $\nu_3$ mode at $2195.633\,\mathrm{cm}^{-1}$ was selected. CO detection was performed using its R(14) line at $2196.664\,\mathrm{cm}^{-1}$ (the only CO absorption line within the tuning range of the available QC-DFB laser). The laser current required to reach each of these lines and the

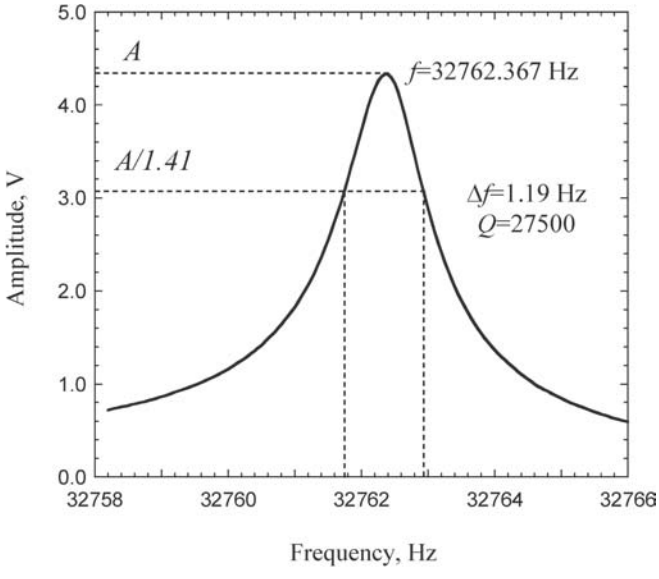


**FIGURE 2** An example of the TF resonance curve. The TF current represented as the lock-in amplifier output is plotted versus frequency of the applied voltage sine wave. The TF is in air at 50 Torr pressure

corresponding laser power inside the TF cell were 590 mA (19 mW) and 493 mA (13 mW), respectively. The accessible CO line was ∼ 2 times weaker in peak absorption than the $N_2O$ line.

## 3 QEPAS and relaxation in gases

Generation of a photoacoustic wave involves the energy transfer from internal to translational molecular degrees of freedom. In the reported experiments a ro-vibrational state is initially excited, which is followed by a collision-induced V-T relaxation. If the vibrational energy excess directly relaxes into an unlimited bath of translational-rotational motions with a time constant $\tau$ (exponential population decay) and the laser input is modulated at a cyclic frequency $\omega = 2\pi f_0$, then the photoacoustic signal $S$ is given by

$$S = S_0 \frac{1}{\sqrt{1+\tan^2\theta}}, \tan\theta = \omega\tau_{VT}(C_{tr}/C_0) \quad (4)$$

where $S_0$ is the photoacoustic signal for instant V-T transfer, $\tau_{VT}$ is the V-T relaxation time constant, $\theta$ is the phase shift between the excitation and photoacoustic signal, $C_{tr}$ is the translational-rotational heat capacity at constant volume, and $C_0$ is the total heat capacity at constant volume [14]. If the relaxation is slow compared to the modulation rate ($\omega\tau_{VT} \gg 1$), then the photoacoustic sound generation is suppressed. Hence, the ability to detect a molecular species by means of PAS does not only depend on its optical absorption strength but is also influenced by the relaxation processes and the radiation modulation frequency.

The influence of relaxation processes on photoacoustic signal is negligible if $\omega\tau \ll 1$ condition is satisfied. Operating at a lower modulation frequency has the additional advantage of a higher photoacoustic signal even for fast-relaxing excited energy levels, because

$$S_0 = \text{const} \times E\frac{\alpha PQ}{f_0} \quad (5)$$

where $\alpha$ is the absorption coefficient, $P$ is the exciting radiation power, and $E$ is a microresonator enhancement factor included in this equation to account for a particular QEPAS sensor design. However, the quartz tuning forks (TF) used as acoustic transducers in QEPAS so far are commercially available only at a resonant frequency of ∼ 32.8 kHz (the modulation frequency in conventional PAS experiments does not usually exceed 4 kHz). Thus, for QEPAS $1/\omega \approx 5$ µs which is comparable to the V-T energy transfer rate in a number of gases and gas mixtures, especially below atmospheric pressure.

In traditional gas-filled resonator based PAS the detection sensitivity increases with pressure, because the resonator $Q$-factor and peak absorption both increase. The effect of pressure on detection sensitivity is different in QEPAS. $Q$ and $E$ were found to be higher at lower pressures, and according to (2), (3) and (5) the signal-to-noise-ratio, SNR ∼ $E\sqrt{Q}$. At the same time $\alpha$ and relaxation rate are decreasing at reduced pressures. The wavelength modulation approach requires the modulation depth to match the absorption line width. Consequently, to determine the optimum conditions for trace gas detection by means of QEPAS, the photoacoustic signal, $S$ has to be mapped as a function of the host gas pressure and the laser modulation depth. In addition, for optimum performance the microresonator length must be adjusted so that its resonant frequency is equal to $f_0$ for the particular host gas composition.

## 4 Experimental results and discussion

### 4.1 *Nitrous oxide* ($N_2O$)

Nitrous oxide is present in ambient air at an almost constant (although location-specific) concentration of ∼ 315 ppb, which is increasing at a 0.8 ppb/year rate [11]. This fact allowed us to use ambient air as a stable unlimited source of trace $N_2O$ for QEPAS optimization. In order to promote the V-T relaxation of the laser-excited vibrational state of $N_2O$, sulfur hexafluoride ($SF_6$) was added to air in concentrations varying from 0 to 8% by volume. $SF_6$ has a high density of vibrational levels, that creates multiple options for resonant energy transfer in collisions with vibrationally excited molecules and a ladder for subsequent efficient multistep relaxation. Previously $SF_6$ was found to significantly improve the sensitivity of photoacoustic $CO_2$ detection as reported in [15]. Our measurements confirmed that the QEPAS signal following $N_2O$ excitation is considerably larger in the presence of $SF_6$. Figure 3 shows the QEPAS signal detected at the absorption line center as a function of $SF_6$ concentration. Even a 0.5% addition of $SF_6$ resulted in 5.7 times signal enhancement. Too high ( > 30%) percentage of $SF_6$ however caused the QEPAS signal to decrease for the following reasons:

1. Dilution of the air sample;
2. Detuning the microresonator resonance from $f_0$ due to the different speed of sound in $SF_6$ and $N_2$;
3. Increased thermal capacity of the carrier gas [$C_p(SF_6) = 97$ J/(mol K) and $C_p(N_2) = 29$ J/(mol K)]

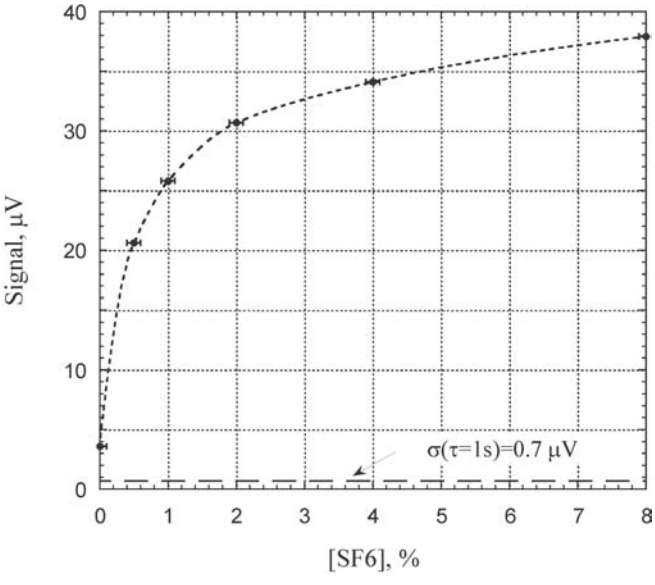


**FIGURE 3** QEPAS signal of $N_2O$ in ambient air (∼ 315 ppb) as a function of added $SF_6$ concentration. Total gas pressure is 50 Torr and laser radiation power in the TF cell is 19 mW

4. Decreased $Q$ of the TF. At 50 Torr pressure the $Q$ was observed to change from 26 600 in pure nitrogen to 10 800 in pure $SF_6$.

In this work a 5% $SF_6$ addition to sampled air was selected as optimum for most $N_2O$ concentration measurements. Higher $SF_6$ concentration levels do not lead to a considerable gain in $S$ but increase the $SF_6$ consumption and can cause sample contamination with impurities that may be present in $SF_6$. Such a $SF_6$ addition gives rise to a 9.8 times signal gain as compared to a $N_2O$ signal from undoped air. The measurements were performed with a gas flow ranging from 50 to 70 standard cubic cm per minute (ccm; $SF_6$ was continuously added using a gas mixer) to avoid adsorption-desorption effects on the precision and accuracy of the experimental results. In Fig. 4 an example of QEPAS spectral data acquired for an ambient air sample with 5% $SF_6$ at a 50 Torr total pressure is shown. The lock-in amplifier time constant was set to 3 s, and the laser power in the TF cell was 11 mW. 50 Torr pressure was found to be optimum for $N_2O$ detection in air or nitrogen.

A NOAA certified Nowat Ridge air sample from a cylinder filled in 1996 containing $313.3 \pm 0.3$ ppbv of $N_2O$ (at the time of filling) was used for the QEPAS sensor calibration. A trace of the sensor readings for this sample (lock mode) followed by a trace for ambient air is shown in Fig. 5. In both cases 5% $SF_6$ was added. The lock-in amplifier time constant was set to $\tau = 1$ s and the measurements were repeated every 3 s. The laser power in the TF cell was 19 mW. The scatter of the results does not depend on the $N_2O$ concentration or the laser power and is in agreement with the calculated thermal noise of the TF [16]. This calibration yields the sensor transfer function 0.101 μV/ppbv for $N_2O$, which in turn yields a room concentration $[N_2O] = 353.5$ ppb and a noise-equivalent detection sensitivity of 7 ppb for a 1 s time constant. The accuracy of the measured room $[N_2O]$ is determined by the accuracy of the calibration gas data. A seemingly too high measured concentration of the $N_2O$ in room air may indicate that some of the $N_2O$ in the air sample collected in 1996 has decomposed. However, if we assume that the calibration is correct, the resulting inaccuracy will not exceed 15%.

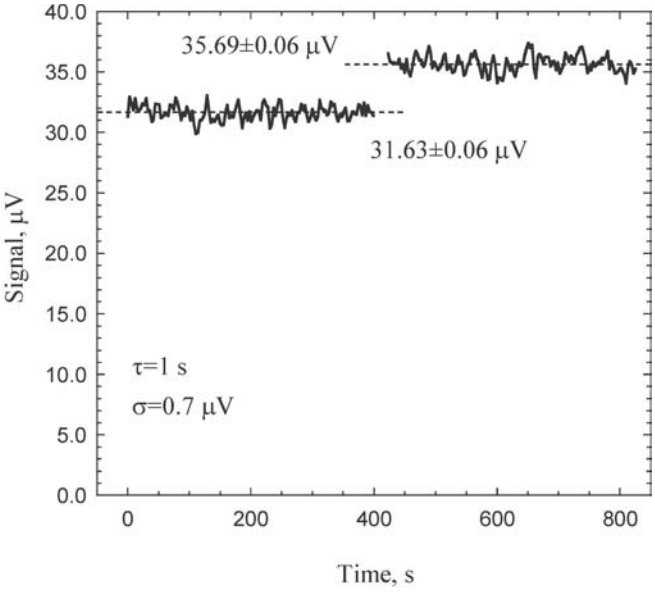


**FIGURE 5** QEPAS signal in lock mode. *First part* (up to ∼ 400 s): a sample of Niwot Ridge Colorado air supplied by NOAA in 1996; *second part*: ambient air

Based on the above calibration, the $N_2O$ concentration in a gas mixture containing ultrapure $N_2$ and 5% $SF_6$ (BOC Gases) was analyzed. The acquired data are presented in Fig. 6. For these measurements the lock-in time constant was increased to $\tau = 3$ s, which resulted in a noise reduction to

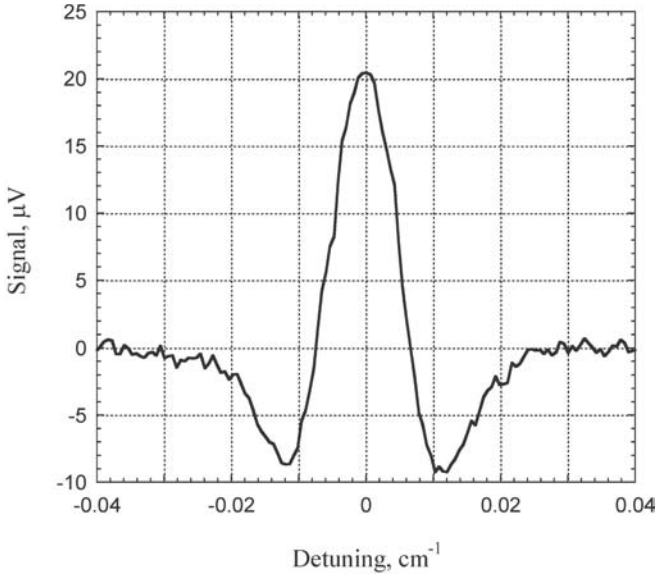


**FIGURE 4** An example of the $N_2O$ absorption line at 2195.633 $cm^{-1}$ detected in ambient air at 50 Torr with QEPAS in a scan mode. Laser power in the TF cell is 11 mW, lock-in amplifier time constant is 3 s, and 5% $SF_6$ introduced to the air sample

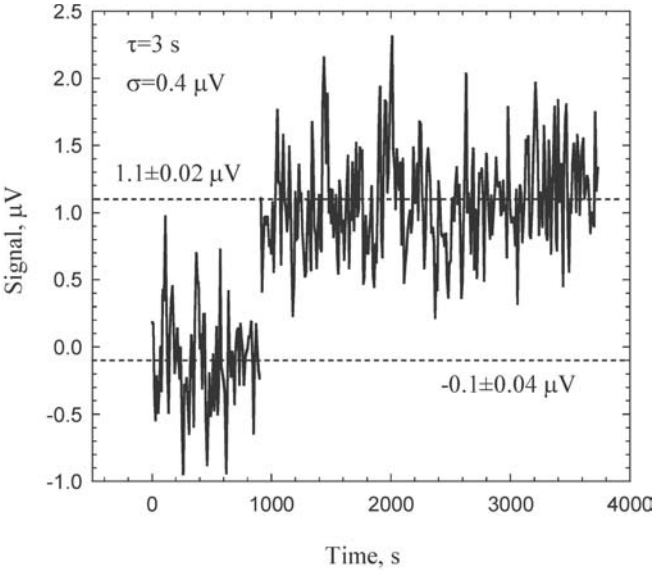


**FIGURE 6** QEPAS signal in lock mode. *First part* (up to ∼ 1000 s): laser wavelength detuned from the absorption line; *second part*: laser is locked to the $N_2O$ absorption line at 2195.633 $cm^{-1}$

0.4 μV, or a 4 ppb single measurement. The measurements were performed every 10 seconds. The initial portion of the plot (i.e. ∼ 1000 s) depicted in Fig. 6 shows the sensor readings when the laser wavelength was shifted off the absorption line (zero signal expected). A small deviation from zero is most probably due to the scattered laser light absorbed in the microresonator tube. The trace beyond 1000 s shows the sensor readings in the lock mode. The observed photoacoustic signal corresponds to 11 ppbv of $N_2O$ in the analyzed gas.

The normalized QEPAS sensitivity $D(N_2O)$ based on the experiments reported above and the HITRAN database is $D(N_2O) = 1.5 \times 10^{-8}\,\mathrm{cm^{-1}W/\sqrt{Hz}}$. This number is ∼ two times higher (meaning lower sensitivity) than $D(NH_3)$ obtained in the near-IR region [3]. Two possible reasons for this are the slower V-T energy transfer in $N_2O$-$N_2$-5%$SF_6$ system and a shift of the microresonator resonance as a result of presence of $SF_6$ ($E$ reduced in (5)). The potential relaxation pathways of the laser-excited $N_2O$ energy level are shown in Fig. 7. When the P(30) line is excited, one rotational quantum ($28\,\mathrm{cm^{-1}}$) is removed from the molecular rotational energy. The first relaxation step is the distribution of this energy deficiency among rotational-translational (R,T) degrees of freedom, resulting in a *cooling* of the gas. Molecular collisions will also result in the following processes:

1. Energy transfer to the $N_2$ molecular vibration. This process can be of significant probability because of the close resonance between the $N_2O$ $\nu_3$ vibration ($2223\,\mathrm{cm^{-1}}$) and $N_2$ vibration ($2331\,\mathrm{cm^{-1}}$). Such energy transfers also result in gas *cooling* because the energy mismatch $\Delta E = -107\,\mathrm{cm^{-1}}$ is borrowed from the bath of R,T motions.
2. Energy transfer to $SF_6$ vibrations. The dense manifold of $SF_6$ ro-vibrational levels ensures close resonance for some levels of $SF_6$ and $N_2O$, as well as facilitates the consequent V-T relaxation down the ladder of vibrational levels.
3. Energy transfer to other vibrational levels of $N_2O$, with the energy mismatch being released to (or absorbed from) the R,T degrees of freedom.
4. Following (1), $N_2$ excitation can be transferred to $SF_6$ molecules with a subsequent V-T relaxation of $SF_6$.

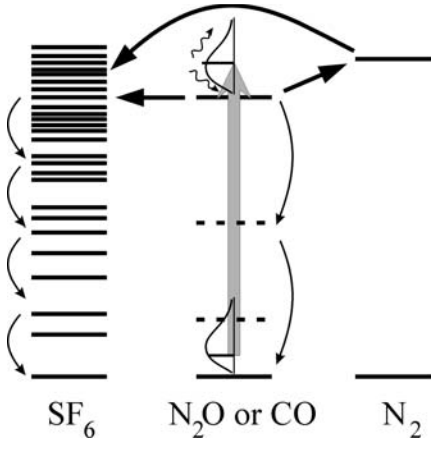


**FIGURE 7** Relaxation pathways following optical excitation (represented by wide gray arrow) of $v = 1$ level of $N_2O$ or CO molecule

Relaxation of $N_2$ in dry air is known to be very slow [17]. Addition of 1% $H_2O$ increases the relaxation rate 30 times, but even in this case and atmospheric pressure the relaxation time $\tau_{VT}(N_2) = 710\,\mu s$ and is much longer than $1/\omega = 5\,\mu s$. Therefore, it is likely that some energy irreversibly leaks from $N_2O$ to $N_2$ and becomes excluded from the photoacoustic signal generation (so-called ''kinetic cooling''). This process can contribute to the decrease in QEPAS sensitivity as compared to $NH_3$ near-IR detection along with a reduced $Q$-factor and microresonator resonance shift caused by $SF_6$ addition to the sampled gas.

### 4.2 *Carbon monoxide (CO)*

The QEPAS signal obtained with the excitation of the R(14) transition of CO molecules in $N_2$ as a host gas at 50 Torr total pressure was found to be 35 times weaker than the signal produced by an equally absorbing amount of $N_2O$ in $N_2$:5%$SF_6$ [normalized to laser power: $D(CO) = D(N_2O)/35$]. Consequently, the QEPAS-based sensor was 70 times less sensitive to CO in terms of concentration than to $N_2O$. Unlike for $N_2O$ detection, the addition of up to 10% of $SF_6$ did not result in a substantial sensitivity improvement. If the total pressure was increased up to 1 atm, the sensor response to CO followed the gradual decrease of the TF $Q$-factor. Thus, the single-measurement noise-equivalent sensitivity of QEPAS to CO at $\tau = 3$ s was 280 ppbv, which was not sufficient to monitor atmospheric CO.

Direct V-T energy transfer from vibrationally excited CO in a CO:$N_2$ mixture is known to be a slow process and can therefore be excluded from consideration on $1/\omega$ time scale. The fastest relaxation process following CO excitation is the rotational equilibration resulting in the release of $53\,\mathrm{cm^{-1}}$ [one rotational quantum for R(14) transition] of the total $2197\,\mathrm{cm^{-1}}$ per excited molecule. According to (4), the rotational equilibration will result in the photoacoustic signal with $\theta \approx 0$ and amplitude

$$S_R = S_0^i \frac{53\,\mathrm{cm^{-1}}}{2197\,\mathrm{cm^{-1}}} \approx S_0^i/40 \tag{6}$$

Here $S_0^i$ is a PAS signal that would be generated if all the absorbed optical energy is instantly released to translational motion of the gas molecules.

The next fastest process is the resonant energy transfer to $N_2$ molecules. The rate constant for this reaction was experimentally measured [18], and gives a relaxation time $\tau(CO-{}^{14}N_2) = 110\,\mu s$ if scaled to a 50 Torr pressure. Each reactive collision results in borrowing $187\,\mathrm{cm^{-1}}$ from the R,T bath to compensate for the energy mismatch, thus cooling down the gas. From (4) it follows that for this process $\tan\theta \approx 23$. The corresponding photoacoustic signal is

$$S_{CO-N_2O} = S_0^i \frac{187\,\mathrm{cm^{-1}}}{2197\,\mathrm{cm^{-1}}} \frac{1}{\sqrt{1+23^2}} \approx S_0^i/270 \tag{7}$$

and is shifted in phase almost 90° with respect to $S_R$.

Consequently the net photoacoustic signal resulting from these two fastest energy transfer channels in a CO:$N_2$ mixture is practically equal to $S_R \approx S_0^i/40$. As $D(CO) = D(N_2O)/35$, we can conclude that:

1. $N_2O$ V-T relaxation time in a $N_2$:5%$S_6$ host at 50 Torr $\tau(N_2O) < 0.6/\omega$ [i.e. $\tau(N_2O) < 3\,\mu s$], following from the condition that $\frac{1}{\sqrt{1+\tan^2\theta}} > \frac{35}{40}$;
2. the observed photoacoustic signal in a CO:$N_2$ mixture at 32.8 kHz is mostly the result of rotational relaxation. V-T energy transfer in this system is too slow to produce a measurable photoacoustic response at this modulation frequency.

## 5 Conclusions

This work demonstrated that the QEPAS technique can be successfully used for ultra-sensitive detection of trace gas species excited to $v = 1$ vibrational levels. The realized sensitivity to absorption $D(N_2O) = 1.5 \times 10^{-8}\,cm^{-1}W/\sqrt{Hz}$ allowed the detection of $N_2O$ in air and nitrogen samples with a 4 ppbv noise-equivalent ($1\sigma$) sensitivity and 3 s response time to $(1 - 1/e)$ of the steady-state level. However, the results of our experiments indicate that V-T energy transfer from $v = 1$ excited level of simple molecules is slower than the relaxation of overtone vibrations [3, 4]. In some cases the relaxation rate can be enhanced by adding an appropriate species to the gas sample (e.g., $SF_6$ added to $N_2$ for $N_2O$ detection). The vibrational relaxation of CO was found to be too slow to produce a measurable QEPAS signal. Nevertheless, we were able to detect this molecule with 280 ppbv noise-equivalent sensitivity due to the rotational relaxation related signal. Thus, a sensitivity improvement of only a few times (via higher laser power or by the means as discussed in the following paragraph) will make the QEPAS sensor reported in this work useful for atmospheric CO monitoring. $SF_6$ does not significantly promote vibrational deexcitation of CO, although it is efficient in case of $N_2O$. This suggests the involvement of lower vibrational levels of the $N_2O$ molecule in V-T energy transfer.

We expect that refinement of the microresonator design and fabrication technology will lead to a considerable gain in QEPAS sensitivity. Future designs will minimize the openings at the junctions of the resonator tubes and TF, which will ensure better confinement of the photoacoustic sound waves. Another approach to better QEPAS detection sensitivity is to develop a custom-made TF with lower resonant frequency. The desired frequency shift can be achieved by adding compact weights to the ends of a standard 32.8 kHz TF. If this is done properly, only the parameter $L$ will change in (3). It can be seen from (2), (3) and (5) that SNR will scale as $f_0^{-3/2}$. Thus, if the weights shift the TF frequency from 32.8 kHz to 10 kHz, the QEPAS sensitivity should theoretically increase 6 times, even if the V-T relaxation is instant.

**ACKNOWLEDGEMENTS** The authors acknowledge helpful discussions with Prof. Robert F. Curl. The quantum cascade laser used in this work was kindly provided by Alpes Lasers. We would also like to thank Dr. E. Dlugokencky of NOAA for providing Nowat Ridge certified air sample. The authors gratefully acknowledge financial support from the National Aeronautics and Space Administration, the Texas Advanced Technology Program, the Robert Welch Foundation, and the Office of Naval Research via a subaward from Texas A&M University.

## REFERENCES

1 A.A. Kosterev, Y.A. Bakhirkin, R.F. Curl, F.K. Tittel: Opt. Lett. **27**, 1902 (2002)
2 F.G.C. Bijnen, F.J.M. Harren, J.H.P. Hackstein, J. Reuss: Appl. Opt. **35**, 5357 (1996)
3 A.A. Kosterev, F.K. Tittel: Ammonia detection using quartz-enhanced photoacoustic spectroscopy with a near-IR telecommunication diode laser, accepted for publication in Appl. Opt.
4 D. Weidmann, A.A. Kosterev, F.K. Tittel, N. Ryan, D. McDonald: Application of widely electrically-tunable diode laser to chemical gas sensing with quartz-enhanced photoacoustic spectroscopy, Opt. Lett. **29**, 1837 (2004)
5 A.A. Kosterev, Y.A. Bakhirkin, F.K. Tittel, S. Blaser, Y. Bonetti, L. Hvozdara: Appl. Phys. B **78**, 673 (2004)
6 D.C. Scott, R.L. Herman, C.R. Webster, R.D. May, G.J. Flesch, E.J. Moyer: Appl. Opt. **38**, 4609 (1999)
7 C.R. Webster, G.J. Flesch, D.C. Scott, J.E. Swanson, R.D. May, W.S. Woodward, C. Gmachl, F. Capasso, D.L. Sivco, J.N. Bailargeon, A.L. Hutchinson, A.Y. Cho: Appl. Opt. **40**, 321 (2001)
8 G. Wetzel, H. Oelhaf, R. Ruhnke, F. Friedl-Vallon, A. Kleinert, W. Kouker, G. Maucher, T. Reddmann, M. Seefeldner, M. Stowasser, O. Trieschmann, T. von Clarmann, H. Fischer: J. Geophys. Res. **107**(D16), 10.1029/2001JD000916 (2002)
9 M.H. Proffitt, K. Aikin, A.F. Tuck, J.J. Margitan, C.R. Webster, G.C. Toon, J.W. Elkins: J. Geophys. Res. **108**, 4110 (2003)
10 G. Kopp, H. Berg, T. Blumenstock, H. Fischer, F. Hase, G. Hochschild, M. Höpfner, W. Kouker, T. Reddmann, R. Ruhnke, U. Raffalski, Y. Kondo: J. Geophys. Res. **108**, 8308 (2003)
11 R.J. Martin: Nitrous oxide measurements in clean air, Proceedings of the Workshop on the Science of Atmospheric Trace Gases, ed. by T.S. Clarkson, NIWA Technical Report 15, p.115 (1998)
12 T. Holloway, H. Levy II, P. Kasibhatla: J. Geophys. Res. **105**, 12 123 (2000)
13 S.A. Kharitonov, P.J. Barnes: Am. J. Respirat. Critic. Care Med. **163**, 1693 (2001)
14 T.L. Cottrell, J.C. McCoubrey: *Molecular energy transfer in gases* (Butterworths, London 1961)
15 M. van Herpen: Continuous-wave optical parametric oscillator for trace gas detection in life sciences, Ph.D. Thesis, Katholieke Universiteit Nijmegen, Netherlands (2004) Chapt. 10
16 R.D. Grober, J. Acimovic, J. Schuck, D. Hessman, P.J. Kindlemann, J. Hespanha, A.S. Morse, K. Karrai, I. Tiemann, S. Manus: Rev. Sci. Instrum. **71**, 2776 (2000)
17 R.A. Rooth, A.J.L. Verhage, L.W. Wouters: Appl. Opt. **29**, 3643 (1990)
18 D.C. Allen, C.J.S.M. Simpson: Chem. Phys. **45**, 203 (1980)